

Abstract

Laser Shock Processing (LSP) has been demonstrated as an emerging technique for the induction of RS's fields in sub-surface layers of relatively thick specimens. However, the LSP treatment of relatively thin specimens brings, as an additional consequence, the possible bending in a process of laser shock forming. This effect poses a new class of problems regarding the attainment of specified RS's depth profiles in the mentioned type of sheets, and, what can be more critical, an overall deformation of the treated component.

The analysis of the problem of LSP treatment for induction of tentatively through-thickness RS's fields for fatigue life enhancement in relatively thin sheets in a way compatible with reduced overall workpiece deformation due to spring-back self-equilibration is envisaged in this paper.

The coupled theoretical-experimental predictive approach developed by the authors has been applied to the specification of LSP treatments for achievement of RS's fields tentatively able to retard crack propagation on normalized specimens. A convergence between numerical code results and experimental results coming from direct RS's measurement is presented as a first step for the treatment of the normalized specimens under optimized conditions and verification of the crack retardation properties virtually induced.

1 Introduction

The capability of Laser Shock Processing (LSP) for the induction of residual stress fields in sub-surface layers of relatively thick specimens ($d > 6$ mm) in view of the improvement of their fatigue life has been widely demonstrated [1-4]. However, the LSP treatment of relatively thin specimens (normally $d < 6$ mm, but also thicker ones depending on the treatment intensity) brings, as an additional consequence, the possible bending of the treated specimen, a feature that can otherwise be employed for forming procedures according to the laser shock forming process.

This effect poses a new class of problems regarding the attainment of specified residual stress depth profiles in the treated specimens, as their self-equilibration reaction after clamping removal can considerably alter the primary laser shock induced residual stress fields, thus possibly motivating undesired final residual stress field distributions, and, what can be more critical, an overall deformation of the treated component. A similar kind of problems has been analyzed for the case of Shot Peening by Guagliano [5]

With the aid of the calculational system developed by the authors (SHOCKLAS®; see [6-7]), the analysis of the problem of LSP treatment for induction of residual stress fields for fatigue life enhancement in relatively thin sheets in a way compatible with reduced overall workpiece deformation due to spring-back self-equilibration has been envisaged. Numerical results directly tested against experimental results have been obtained confirming the critical influence of the laser energy and irradiation geometry parameters.

2 Problem definition and theoretical/experimental methodology

The fatigue life of a component depends upon the crack initiation and growth caused during usage. In many structural applications, cracks begin at the surface, leading to fatigue failure. The component fatigue life depends upon the surface and near-surface stress field generated by the loading conditions. The effects of surface and near-surface tensile stress can be mitigated by generating compressive residual stress fields at possible crack locations on the surface.

LSP is based on the application of a high intensity pulsed laser beam (Instant peak power density, $I > 1 \text{ GW/cm}^2$; Laser pulse characteristic duration, $\tau < 50 \text{ ns}$) at the interface between the metallic target and the surrounding medium (a transparent confining material, normally water) forcing a sudden vaporization of the metallic surface into a high temperature and density plasma that immediately develops inducing a shock wave propagating into the material [2]. This shock wave induces plastic deformation and a residual stress distribution in the target material (if its peak pressure is greater than the dynamic yield limit) able to protect the component by means of a compressive residual stresses (RSs) field.

However, in view of the particular (not trivial) mode in which the stress distribution is altered inside the treated material by the LSP treatment and the possible associate problems due to component deformation, the way in which this effect must be achieved is not direct and is the object of the present investigation.

In this section, the main details of the LSP irradiation strategy, experimental procedure and numerical simulation tools used for the analysis are presented.

2.1. Laser irradiation geometry and pulse overlapping strategy

Plane rectangular specimens (160 mm x 100 mm x 2 mm) of Al-cladded ($\sim 80 \mu\text{m}$) Al2024-T351 (Young Modulus, $E=72 \text{ GPa}$, Yield Strength; $YS = 360 \text{ MPa}$; Poisson ration, $\nu = 0.33$; Density, $\rho=2780 \text{ kg/m}^3$) were considered both for LSP experimental treatment and for corresponding numerical simulation. In figure 1 the practical geometry considered for the LSP simulations is displayed showing the references used for the directions of evaluation of residual stresses. The figure also shows the pulse overlapping and specimen sweeping strategy used in the irradiation.

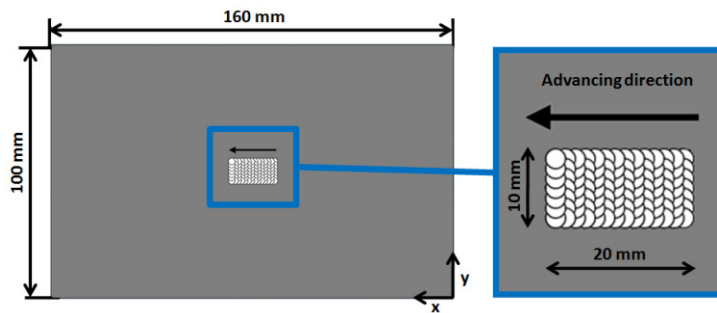


Figure 1. Practical geometry considered in the LSP simulations in which the residual stresses reference axes are attributed.

2.2. Experimental procedure

The practical irradiation system used for the LSP experiments is schematically and photographically shown in figure 2.

The laser source is a Q-switched Nd:YAG pulsed laser working in fundamental mode ($\lambda = 1064 \text{ nm}$) and at a repetition rate of 10 Hz. The FWHM (full width at half maximum) of the generated pulses is about 9 ns and the maximum pulse energy is 2.4 J/pulse. Using a flat mirror and a convergent lens, the laser pulse is focused on the target. Both optical components are coated for 1064 nm, what guarantees high transmittance efficiency. The convergent lens is used to control the transmitted laser energy. The laser interaction with the target is confined by a thin water layer and no protective coating is applied. Control of water purity is important in order to avoid the formation of water bubbles or the concentration of impurities coming from the material ablation due to laser treatment. The appearance of suspended elements can affect the LSP process by their interaction with the high-energy laser beam.

The test piece is fixed on a holder and is driven along X and Y directions by means of an anthropomorphic robot. The predefined pulse overlapping strategy is used for the irradiation of extended areas of material.

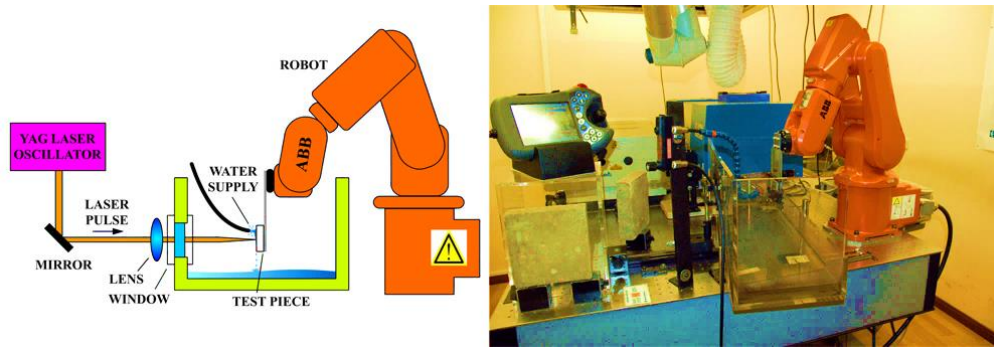


Figure 2. Schematic representation and photographic view of the LSP irradiation experimental setup used in experiments.

In table 1, the main laser irradiation parameters used for the analysis are shown for two characteristic values found by the authors to produce the sought through-thickness Residual Stresses profiles in the considered plates (see ref [8]) defined in terms of pulse overlapping pitch and laser pulse diameter according to the definitions found in ref [9]. The Equivalent Overlapping Density (EOD) indicates the number of individual pulses per unit surface, the Equivalent Energy Density (EED) indicates the final energy that the unit surface has received along the treatment and the Equivalent Local Overlapping Factor (ELOF) indicates the average number of LSP pulses applied on a particular surface location.

Table 1.: Summary of laser irradiation parameters for two characteristic LSP treatments applied to the defined thin Al2024-T351 specimens

Treatment condition	Laser pulse energy, E (J)	Laser pulse overlapping distance, d (mm)	Laser spot diameter, Ø (mm)	Equivalent Overlapping Density, EOD (1/cm ²)	Equivalent Energy Density, EED (J/cm ²)	Equivalent Local Overlapping Factor, ELOF ()
A	2.4	0.75	1.50	178	427	3.14
B	2.4	0.75	2.50	178	427	8.73

2.3. Numerical modeling

In order to predictively assess the LSP treatment results, the numerical model SHOCKLAS® developed by the authors has been applied to the simulation of the selected treatments

SHOCKLAS® is a complex calculational system analyzing the laser-material interaction at the used high laser intensity, including the associate plasma formation and solves the shock wave propagation problem into the solid material with specific consideration of its elastic-plastic behavior [10]. The mechanical behavior analysis module (HARDSHOCK-3D) is based in the finite element model commercial code ABAQUS [11].

From the geometrical point of view, a full 3D configuration for the real geometry and for the sequential overlapping strategy of pulses has been considered. The FEM elements used for the simulation are an eight-node brick reduced integration with hourglass control in the treated area, namely C3D8RT, and a six-node triangle prism in the rest of the geometry, where there is no applied load, namely C3D6T. This makes more easy the meshing of the different scales in the complex partitions. The element size in the nearest of the treated surface is 100 x 100 x 25 µm, being the maximum element size which allows to maintain calculation convergence.

In LSP processes, the material is stressed and deformed in a dynamic way, with strain rates exceeding 10^6 s^{-1} , so the elasto-plastic behavior of Al2024-T351 is modeled using Johnson-Cook equation [12] fitted with Kay parameters [13].

3. Results

In this section, results relative to the two most relevant aspects of the considered problem are presented, namely the analysis of the local/global deformation by LSP (predictive numerical simulation results) and the induction of through-thickness compressive residual stresses fields (numerical simulation results compared to experimental determinations).

3.1. Numerical Analysis of Local/Global plates deformation

Although generally not considered in the LSP treatment of thick pieces, the deformation in thin plates is a relevant aspect to be taken into account in order not to negatively affect the pursued effect of induction of compressive residual stresses in the treated specimens.

In view of this relevance the SHOCKLAS® model has been applied to the determination of the deformation induced by the LSP treatment in the considered specimens. Both longitudinal (path \underline{x} in figure 4) and transverse (path \underline{y} in figure 3) deformations of the simulated plate have been evaluated for LSP treatment conditions showed in table 1.

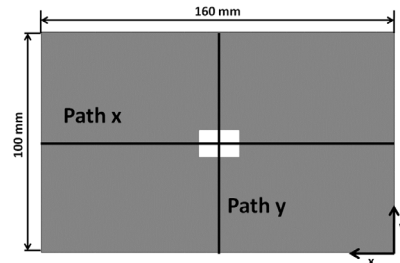


Figure 3. Defined paths for analysis of LSP induced deformation.

In order to show the qualitative behaviour of the considered deformation, in figure 4 an augmented scale (x 50) 3D simulation view is shown in which the described effect is clearly shown for the case of a long (100 mm) LSP treated stripe with parametric conditions A.

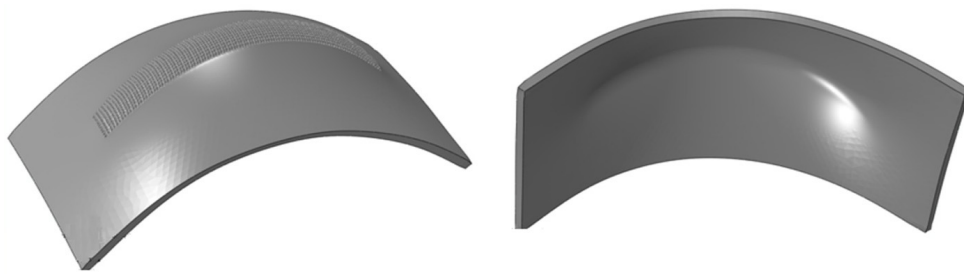


Figure 4. Augmented scale (x50) 3D simulation view of the LSP-induced deformation in a thin Al2024-T351 plate

Comentario [JLOM1]: Figure 4 changed

Quantitative deformation results for the two selected LSP parametric conditions are shown in figures 5 (left and right), each of them corresponding to one of the selected paths (\underline{x} and \underline{y}). Results show substantial effects after LSP treatments both at the local and global scales and it can be clearly observed that modification in the LSP parameters imply changes in the generated deformations.

Specifically, it can be observed how a larger ratio between the laser beam diameter, \varnothing , and the pulse spacing (finally accounted by the ELOF parameter in table 1) leads to more favourable (lower level) deformations, both at the local and global scales, the effect being most pronounced at the local scale, which is the most critical from the point of view of induction of compressive residual stresses fields at points close to the plate surface. The additional fact that the global scale deformation for higher values of the ELOF parameter is generally lower (except possibly for the plate lateral edges, as shown in figure 7) provides an important condition that can be used for the global scale overall deformation compensation by double side plate treatment, a technologically relevant possibility as shown in the next section.

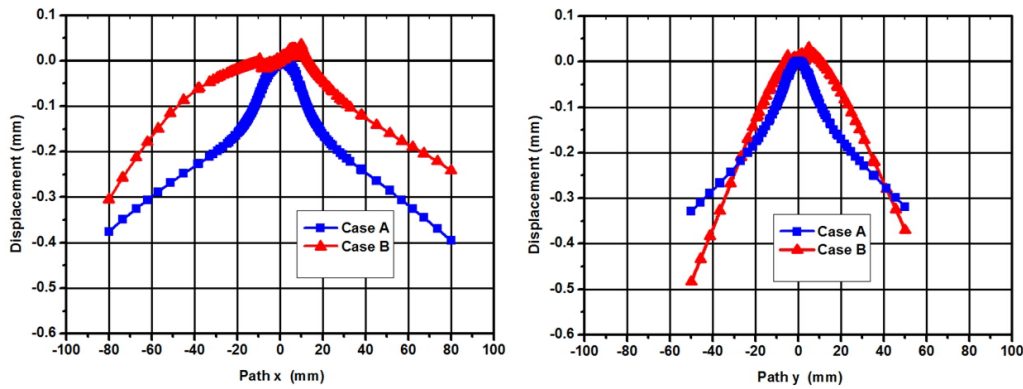


Figure 5. Comparison between deformations along paths \underline{x} (left) and \underline{y} (right) for parametric conditions A and B.

3.2. Residual stress fields

As a main objective envisaged by the LSP treatment, compressive residual stresses fields in a given depth below the treated surface are sought. In the case of thin plates, the induction of these fields must be compatible both with a given limit in deformation and with a given limit in the tensile residual stress induced at the surrounding zones of the treated zones.

According to the results of section 3.1, a compromise between the EOD (assuring a minimum value of compressive residual stress) and ELOF (assuring a limited plate distortion) parameters must be found.

In figures 6 (left and right), an analysis is provided based on numerical simulation results on the surface residual stresses along the defined \underline{x} and \underline{y} directions for different combined values of the laser beam diameter, ϕ , and the overlapping pitch, d , the main conclusion being that, for overlapping pitches in the range of $d=0.75$ (a practical value experimentally found providing at least a minimum level of compressive residual stresses), beam diameters around $\phi=2.5$ are preferable for induction of higher values of these stresses in both perpendicular directions.

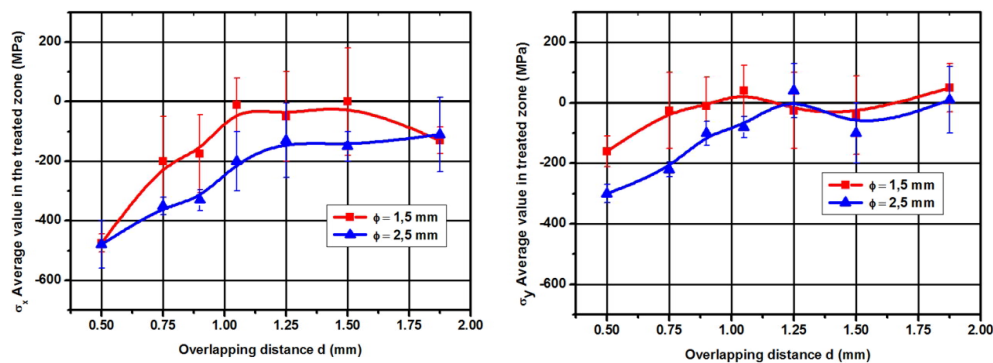


Figure 6. Variation of surface average value of σ_x (left) and σ_y (right) components of RS's (according to reference in figure 1) in a transverse profile (\underline{y} direction) for different values of ϕ - d parametric space combinations (uncertainty bars indicate oscillations around average value).

Comentario [JLOM2]: Note to Reviewer 1 (comment 11): It is not the object of this part of the paper to compare the results on deformation with experimental ones but just to prevent about the possibility of deformation and show the possibility of smearing it with change of the processing parameters. By the contrary, the comparison of experimental residual stresses to numerically calculated is made in the next section.

Comentario [JLOM3]: Figure 5 changed

Comentario [JLOM4]: Figure 6 changed

With these data in mind, the final envisaged objective is the achievement of through-thickness compressive residual stresses profiles and this possibility has been both numerically and experimentally explored.

With the aid of the SHOCKLAS® simulation code, different parametric variations around the reference provided by the condition B in table 1 and the corresponding results have been obtained. In figures 7 (left and right) numerical simulation results are shown of the final residual stress state (in both perpendicular \underline{x} and \underline{y} directions) in a middle transverse cut (\underline{y} direction) of the considered geometry. It is clearly observed how the plate front (direct laser beam incidence) is clearly in compressive residual stress and how the rear part of the plate is also under compressive residual stress (in both components), what in practice demonstrates the possibility of induction of the desired through-thickness compressive residual stress fields in selected treated areas that can be supported by adjacent areas concerning RS's global equilibrium.

This has been confirmed by the analysis of complete numerical through-thickness results. As a sample, in figure 8, the variation along the normal to the plate surface in a given position of the treated zone is shown for the referred parametric conditions (case B in table 1) and a related case with the same laser beam diameter and an only slightly changing displacement pitch $d=0.9$ mm (this choice of parameters has been chosen only to show the difference with the reference case B).

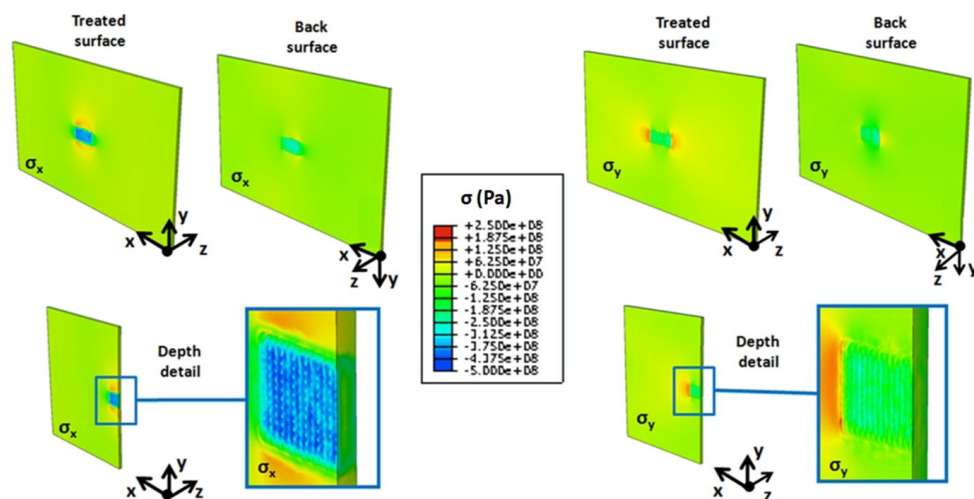


Figure 7. Representation of σ_x (left) and σ_y (right) components of the residual stresses fields in a treated specimen under the B set of parametric conditions.

Comentario [JLOM5]: Figure 7 changed

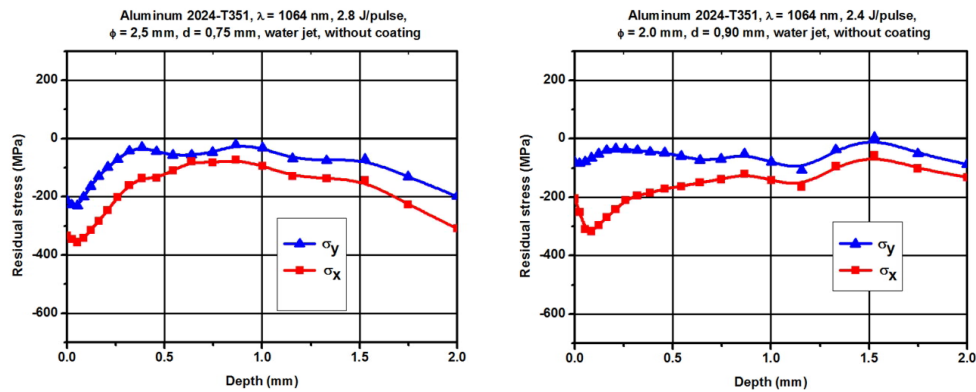


Figure 8. In depth variation of residual stresses components in a representative point of a zone treated by LSP with parametric conditions B (left; $\varnothing=2.5$ mm, $d=0.75$ mm) and other close parameters (right; $\varnothing=2.0$ mm, $d=0.9$ mm).

Comentario [JLOM6]: Figure 8 changed

As a step forward for the practical demonstration of the capability for the induction of through-thickness compressive residual stress fields in the considered thin plates, the generation of these residual stress fields has been experimentally accomplished and the results obtained have been checked against the numerical results provided by the SHOCKLAS® model.

In figure 9, a detail of the positioning of the residual stresses measurement gauges around the treated zone of the considered specimens is presented. In this case, the treated zone is 100 x 10 mm in order to provide room enough for the placement of residual stresses measurement gauges. Experimental residual stresses measurements is performed at the treated surface points and surrounding areas obtaining in-depth profiles (only to a maximum of 1.0 mm depth in order no to exceed the applicability limitations of the method) by means of the hole drilling method (ASTM E837-08 Standard [14]).



Figure 9. Detailed view of the positioning of the strain gauges for the determination of in-depth residual stresses fields according to ASTM E837 08 standard.

Comentario [JLOM7]: Old Figure 9 suppressed.

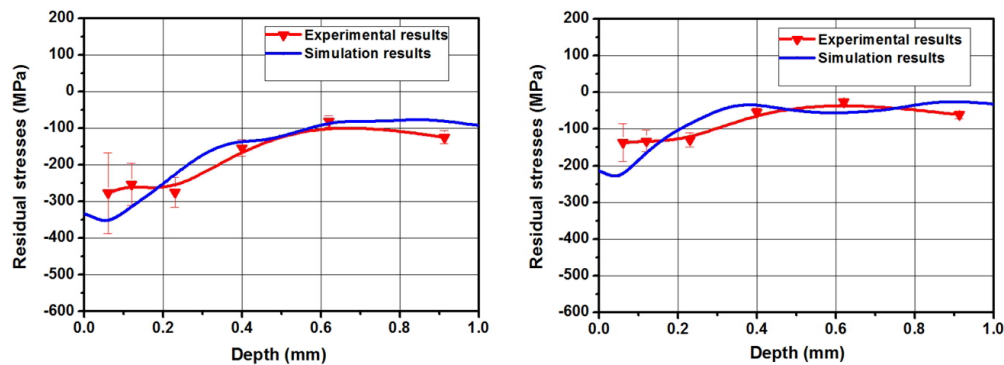


Figure 10. In depth variation of numerically predicted and experimental values of σ_x (left) and σ_y (right) components of residual stresses fields induced by LSP treatment under parametric conditions B in point 1.

Comentario [JLOM8]: Figure 10 (Old 11) changed

In figures 10 (left and right), i.e., simulation results corresponding to residual stresses fields along the two defined perpendicular directions (x and y) are presented respectively for the defined LSP treatment conditions B in point 1 along with the corresponding experimental data obtained according to the referred ASTM standard. To be noticed the effective induction of compressive residual stresses and the very good agreement of numerical predictions and experimental values.

Although in the selected case of parametric conditions B the achieved residual stress distribution field is quite satisfactory through the complete plate thickness for the concrete analysis point reported in previous figures, this is not unfortunately the case for other parametric combinations or for other points over the same treated surface, so that, in order to assure a minimum value of compressive residual stress across this thickness, the double side treatment of the plates has also been investigated.

In figures 11 (top and bottom), the slight but positive effect of the double-side treatment can be appreciated in the simulation results corresponding to a sample with both single-side (a) and double-side (b) treatments.

From an analytical point of view, in figure 12 numerical simulation results are presented showing the effect of the double-side treatment in both perpendicular components of residual stresses for a given point (point 1 in figure 11) of a sample treated with the reference parametric conditions B.

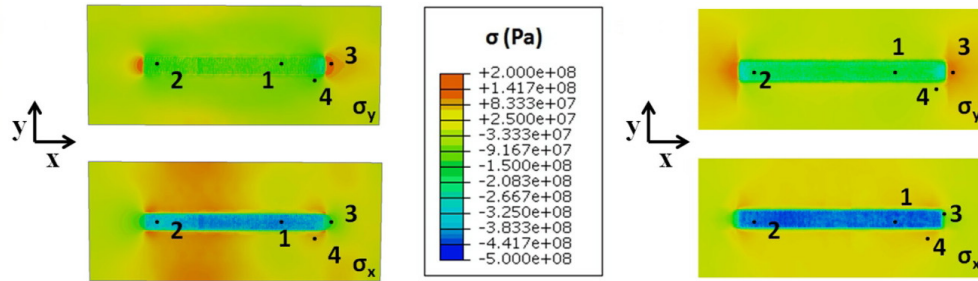


Figure 11. Representation of σ_x and σ_y components of calculated residual stresses in the front and rear sides of single-side (left) and double-side (right) LSP treated specimens. Numbers indicate the position of the control points for measurement of in-depth residual stresses and check against numerical simulation results.

Comentario [JLOM9]: Figure 11 (Old figure 12) changed

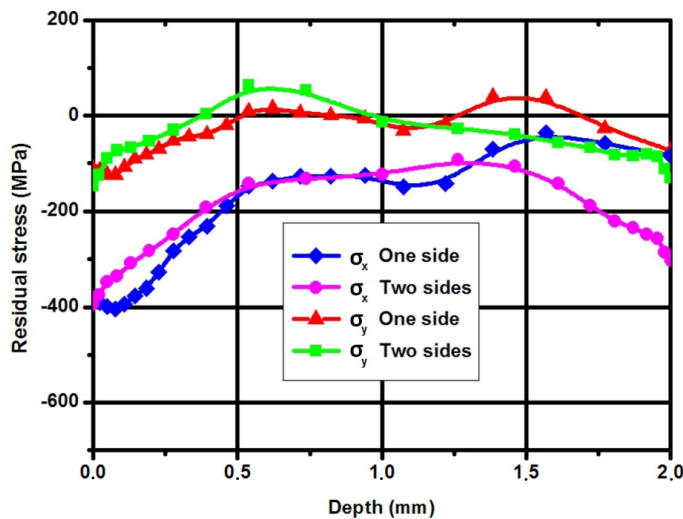


Figure 12. Numerical simulation results showing the effect of double-side treatment on the σ_x and σ_y components of the residual stresses induced through the whole thickness in a point of a LSP treated plate (point 1 in figure 11) with parametric conditions B.

Comentario [JLOM10]: Figure 12 (Old figure 13) changed

Finally, in figure 13, and as a complete verification of the capability of inducing through-thickness compressive residual stress in the considered kind of thin plates, the double-side experimental residual stresses measurement results (needed in view of the maximum range of the ASTM E837-08 standard method) corresponding to one of the defined measurement points are displayed together with the numerical simulation results corresponding to the state of this point, the agreement being again really good.

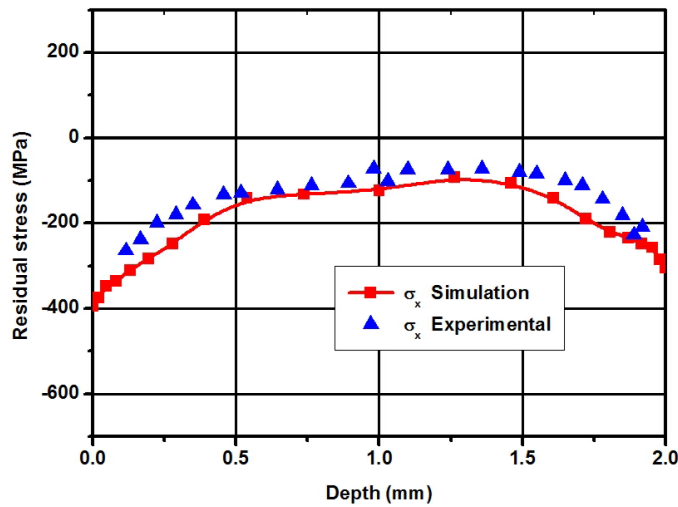


Figure 13. Complete through-thickness experimental residual stresses measurement results compared to corresponding numerical simulation results showing the effect of double-side treatment in a point of a LSP treated plate with parametric conditions B.

Comentario [JLOM11]: Figure 13 (Old figure 14) changed

Although the corresponding study is not included in the present paper (mostly addressed to the demonstration of the possibility of practically inducing through-tickness in the considered kind of specimens), a positive effect (i.e. an important correction of the local+global deformation induced by the one-side treatment) is achieved by means of the double-side treatment, a result that would be expected in view of the more symmetrical distribution of induced residual stresses around the plate mid plane achieved after the second face treatment compared to the first face treatment (as clearly shown in figure 13).

4. Conclusions

The LSP treatment of relatively thin specimens (normally $d < 6$ mm, but also thicker ones depending on the treatment intensity) poses a new class of problems regarding the attainment of specified residual stress depth profiles in the treated specimens, as their self-equilibration reaction after clamping removal can considerably alter the primary laser shock induced residual stress fields, thus possibly motivating undesired final residual stress field distributions, and, what can be more critical, an overall deformation of the treated component.

With the aid of the calculational system developed by the authors, the analysis of the problem of LSP treatment for induction of residual stress fields for fatigue life enhancement in relatively thin sheets in a way compatible with reduced overall workpiece deformation due to spring-back self-equilibration has been envisaged.

Numerical results directly tested against experimental results have been obtained confirming:

- i) The critical influence of the laser energy and irradiation geometry parameters on the possible thin sheets deformation, both at local and global scales.

- ii) The possibility of finding LSP treatment parameter regimes that, maintaining the requirements relative to in-depth residual stresses fields are able to reduce the relative importance of sheet deformation.
- iii) The possibility of finding LSP treatment parameter regimes able to provide through-thickness compressive residual stresses fields **in selected zones** at levels compatible with an effective fatigue life enhancement **due to critical stress concentration zones by using an appropriate residual stresses redistribution in the adjacent zones**.
- iv) The possibility of improving this through-thickness compressive residual stresses fields by double-side treatments **that, in turn, are able to partly correct the possibly important local+global plate deformation induced by a one-side treatment**.
- v) The capability of the experimental LSP treatment system at the authors site (CLUPM) of practically achieve the referred through-thickness compressive residual stresses fields in excellent agreement with the predictive assessment obtained by the used numerical code (SHOCKLAS®).

The referred results provide a firm basis for the design of LSP treatments able to confere a broad range of residual stresses fields to thin components aiming the extension of their fatigue life, an enormously relevant field in which the authors are currently working.

Acknowledgements: Work performed under national Spanish funding (MAT2012-37782)

References

- [1] CLAUER, A.H.: *"Laser shock peening for fatigue resistance"*. Surface Performance of Titanium, J. K. Gregory, H. J. Rack, D. Eylon (eds.). TMS, Warrendale (PA, USA), pp. 217-230 (1996).
- [2] PEYRE, P., FABBRO, R., MERRIEN, P., LIEURADE, H.P.: *"Laser shock processing of aluminium alloys. Application to high cycle fatigue behavior"*. Materials Science and Engineering A, 210, 102-113 (1996).
- [3] RUBIO-GONZÁLEZ, C., FÉLIX-MARTÍNEZ, C., GÓMEZ-ROSAS, G., OCAÑA, J.L., MORALES, M., PORRO, J.A.: *"Effect of laser shock processing on fatigue crack growth of duplex stainless steel"*. Materials Science and Engineering A, 528, 914-919 (2011).
- [4] SANO, Y., MASAKI, K., GUSHI, T., SANO, T.: *"Improvement in fatigue performance of friction stir welded A6061-T6 aluminum alloy by laser peening without coating"*. Materials and Design, 36, 809-814 (2012).
- [5] GUAGLIANO, M.: *"Relating Almen intensity to residual stresses induced by shot peening: a numerical approach"*. Journal of Materials Processing Technology, 110, 277-286 (2001)

- [6] OCAÑA, J.L., MORALES, M., MOLPECERES, C., TORRES, J.: “Numerical simulation of surface deformation and residual stresses fields in laser shock processing experiments”. *Applied. Surface Science*, 238, 242-248 (2004).
- [7] OCAÑA, J.L., MORALES, M., MOLPECERES, C., TORRES, J., PORRO, J.A., GOMEZ-ROSAS, G., RUBIO-GONZÁLEZ, C.: “Predictive assessment and experimental characterization of the influence of irradiation parameters on surface deformation and residual stresses in laser shock processed metallic alloys”. *SPIE Proceedings*, Vol. 5448, 642-653 (2004).
- [8] CORREA, C., RUIZ DE LARA, L., DÍAZ, M., PORRO, J.A. GARCÍA-BELTRÁN, A., OCAÑA, J.L.: “Influence of pulse sequence and edge material effect on fatigue life of Al2024-T351 specimens treated by laser shock processing”. *International Journal of Fatigue* 70, 196–204 (2015).
- [9] OCAÑA, J.L., PORRO, J.A., DÍAZ, M., RUIZ DE LARA, L., CORREA, C., GIL-SANTOS, A., PERAL, D.: “Induction of Engineered Residual Stresses Fields and Enhancement of Fatigue Life of High Reliability Metallic Components by Laser Shock Processing”. *Proc. SPIE 8603, High-Power Laser Materials Processing: Lasers, Beam Delivery, Diagnostics, and Applications II*, 86030D (2013); doi:10.1117/12.2003935.
- [10] MORALES, M., CORREA, C., PORRO, J.A., MOLPECERES, C. OCAÑA, J.L.: “Thermomechanical modelling of stress fields in metallic targets subject to laser shock processing”. *International Journal of Structural Integrity*, 2, 51-61 (2011).
- [11] HIBBITT, KARLSSON, SORESENSEN, INC.: “ABAQUS user’s manual, v. 6.13”. Pawtucket, Rhode Island (2014).
- [12] JOHNSON, G.R., COOK, W.H.: “A constitutive model and data for metals subjected to large strains, high strain rates and high temperatures”, *Proceedings of the 7th International Symposium on Ballistics*, The Hague, pp. 541-547 (1983).
- [13] KAY, G.: “Failure Modeling of Titanium 6Al-4V and Aluminum 2024-T3 with the Johnson-Cook material model”. Technical Report U.S. Department of Transportation, DOT-FAA-AR-97-88, (2003).
- [14] ASTM International.: “ASTM E837-08 Standard Test Method for Determining Residual Stresses by the Hole-Drilling Strain Gage Method”. (2008).